



HAL
open science

Fractal approach to the rheology of concentrated cell suspensions

Andreea Iordan, Alain Duperray, Claude Verdier

► **To cite this version:**

Andreea Iordan, Alain Duperray, Claude Verdier. Fractal approach to the rheology of concentrated cell suspensions. *Physical Review E: Statistical, Nonlinear, and Soft Matter Physics*, 2008, 77, pp.011911. hal-00196481

HAL Id: hal-00196481

<https://hal.science/hal-00196481v1>

Submitted on 12 Dec 2007

HAL is a multi-disciplinary open access archive for the deposit and dissemination of scientific research documents, whether they are published or not. The documents may come from teaching and research institutions in France or abroad, or from public or private research centers.

L'archive ouverte pluridisciplinaire **HAL**, est destinée au dépôt et à la diffusion de documents scientifiques de niveau recherche, publiés ou non, émanant des établissements d'enseignement et de recherche français ou étrangers, des laboratoires publics ou privés.

A fractal approach to the rheology of concentrated cell suspensions

A. Iordan^a, A. Duperray^{b,c}, C. Verdier^{a*}

(a) Laboratoire de Spectrométrie Physique,

CNRS and Université Joseph-Fourier (UMR5588),

140 avenue de la physique, BP87

38402 Saint Martin d'Hères cedex, France.

(b) INSERM, U823, Grenoble, France.

(c) Université Grenoble I – Institut Albert Bonniot,

Centre de Recherche Ontogénèse et Oncogénèse moléculaires,

Grenoble, France.

Abstract

New results on the rheological behavior of CHO cell suspensions in a large range of concentrations are reported. The concentration-dependent yield stress and elastic plateau modulus are formalized in the context of fractal aggregates under shear, and quite different exponents are found as compared to the case of red blood cell suspensions. This is explained in terms of intrinsic microscopic parameters such as the cell-cell adhesion energy and cell elasticity but also the cell's individual dynamic properties, found to correlate well with viscoelastic data at large concentrations ($\phi \geq 0.5$).

PACS numbers: 83.60.La 47.57.Qk 47.57.E- 83.85.Cg

Keywords: rheology, CHO cells, Yield stress, Viscoelasticity, Fractal, aggregates

* Author to whom correspondence should be addressed verdier@ujf-grenoble.fr Tel. +33 4 76 63 59 80 Fax +33 4 76 63 54 95

I. INTRODUCTION

The rheology of complex fluids has been studied extensively over the past decades [1] and has revealed very intriguing behaviors, in particular properties of suspensions, either micronic or colloidal, are still a subject of interest [2, 3, 4, 5]. Classical behaviors of suspensions usually reveal shear–thinning effects, but other unusual ones like shear–thickening [6] (i.e. viscosity increase with shear rate) or yield stress have been observed [2, 3]. The yield stress is the critical value of the shear stress needed to induce flow for a given fluid. It is closely related to the internal structure of the fluid therefore its ability to form (or break) particle clusters under flow. In this respect most studies have focused on solid sphere suspensions.

On the other hand, there are much less works dedicated to suspensions of deformable particles, such as biological cell suspensions. The main works can be found in the field of blood rheology. Suspensions of Red Blood Cells (RBC) within plasma were first investigated by Chien [7, 8] and revealed a shear–thinning behavior, but a more detailed inspection of the viscosity–shear rate diagrams showed that at low shear rates, the stress level is close to a constant σ_s (Pa), called the yield stress. The well–known Casson’s model [9] relating the shear stress σ to the shear rate $\dot{\gamma}$ (μ being a constant viscosity) can be used to determine the yield stress:

$$\sqrt{\sigma} = \sqrt{\sigma_s} + \sqrt{\mu\dot{\gamma}} \quad (1)$$

Chien and co–authors obtained σ_s for a large range of hematocrit (H), i.e. the RBC volume concentration [10]. They showed a relationship of the type $\sigma_s \sim (H - b)^3$ (b being a constant hematocrit).

It is still not known yet whether this type of behavior is universal, or if it could depend on cell type, cell shape or other biological effects such as cell adhesion or cell elasticity. In particular, one proposed explanation of the yield stress in RBCs suspensions is based on the existence of ‘rouleaux’ which build due to cell interactions and exhibit large shape aspect ratios [8] and a fractal dimension D . Therefore it is necessary to apply strong enough stresses in order to break such aggregates, in close relation with the yield stress.

In this work we propose to investigate the rheology of a new cell suspension, consisting of CHO cells (Chinese Hamster Ovary cells) in a large range of concentrations. Such cells

are commonly used in biology, easy to culture, and can be genetically modified to induce different adhesive properties. These cells are spherical when suspended in a culture medium, and organized in a specific manner leading to particular aggregation patterns of fractal type. This leads to the determination of scaling laws based on fractal exponents (for the yield stress σ_s and elastic modulus G_0) which are seen to be non universal but dependent on cell type. The flow curves constitute a basis to test classical empirical models (Bingham, Casson, Herschel–Bulkley models) and other ones [11, 12] based on kinetic theories describing the rupture and formation of particle clusters. The latter ones successfully relate macroscopic effects to microscopic parameters, such as the cell–cell adhesion energy and the cell elasticity. The microscopic parameters that we find match well the ones found in the literature using other techniques. This is important in the context of recent studies related to tumour growth [13, 14, 15] which consider cell assemblies with interactions as well as cell elastic deformations. Furthermore, this study emphasizes the relationship between the dynamic rheological properties of suspensions [16] and the single cell properties.

The paper is organized as follows. In §II, we describe the materials and methods of investigation (i.e. mainly rheometry and microscopy). Then steady shear and dynamic oscillatory shear results are presented in §III. In the light of the typical scaling laws obtained, we suggest the use of the model of Snabre and Mills [11] presented in §IV, to analyze our data, and find the corresponding microscopic parameters. Finally, we present an alternative approach based on structural similarity [17] in §V.

II. MATERIALS AND METHODS

In our model system, adherent CHO cells are grown in culture medium (DMEM containing 10% Fetal Calf Serum) using standard *T75* boxes under proper conditions (37°C , $5\% \text{CO}_2$), until they are detached using trypsin, when they reach a confluency of $\sim 70\%$. Suspended cells are centrifuged at 1200 rpm , a high enough velocity to get a concentrated suspension, but slow enough in order to maintain the cells alive. Cell volume concentration ϕ (i.e. similar to the hematocrit H) is determined accurately after centrifugation in hematocrit tubes containing the CHO cells. Then the right amount of remaining supernatant is removed until the desired concentration is obtained (between 0 and 60%). Different experiments were carried out on a conventional Rheometer (Bohlin Gemini 150). Both steady

shear and oscillatory measurements were made at $T = 20^\circ C$. Due to the large amount of cells needed (we usually require twelve *T75* flasks in order to obtain a volume of roughly 0.3 mL of cells), we chose to use a plate–plate geometry (20 mm diameter) with a small gap (between $400\ \mu\text{m}$ and 1 mm) for the concentrated suspensions whereas the smaller concentrations (below 10%) were tested using the 60 mm cone–plane geometry (2° angle). Typically in our fluid, the suspended cells are spherical and monodisperse with a radius $a \sim 10\ \mu\text{m}$.

III. RESULTS

Experimental results for constant steady state shear rate $\dot{\gamma}$ are presented in Fig.1. The viscosity η is shown to vary over several decades, within shear rates typically between 10^{-3} s^{-1} and 10^3 s^{-1} . In some cases, we limited ourselves to the higher shear rates because of experimental reasons (i.e. steady state not reached). By a first inspection of the curves, we recognize the signature of a yield stress fluid as depicted by the slope close to -1 in the viscosity–shear rate diagram (or equivalently a constant shear stress at low shear rates), especially at the largest concentrations ϕ , which will be particularly of interest here. The existence of this yield stress is attributed to weak interactions which can exist after preparation of the system. Already existing proteins are available on cell membranes and can be recruited to form bonds, leading to particular structure arrangements. This explains the presence of a yield stress related to the formation of such structures. The yield stress is found to depend on volume concentration ϕ in a manner to be discussed later.

A second series of experiments was carried out in order to study the systems under oscillatory strains at frequency f . Small deformations (1% or less) within the linear regime were performed in order to characterize the elastic modulus $G'(f)$ and the loss modulus $G''(f)$. The frequency values were limited to the narrow range corresponding to fast modes, in order to limit a possible time–dependence of the results, due to sedimentation, protein expression, or cluster formation–destruction. We find an interesting behavior as shown in Fig.2. Moduli $G''(f)$ usually prevails over $G'(f)$ at small concentrations (e.g. $\phi = 0.2$), but as ϕ increases, the system becomes elastic with a much larger $G'(f)$. This behavior is the signature of a viscoelastic medium, due to the fact that interactions between elastic cells become effective at large concentrations ($\phi \geq 0.4$). The slow increase of the elastic modulus G' against frequency reveals the presence of a so–called 'elastic plateau' modulus

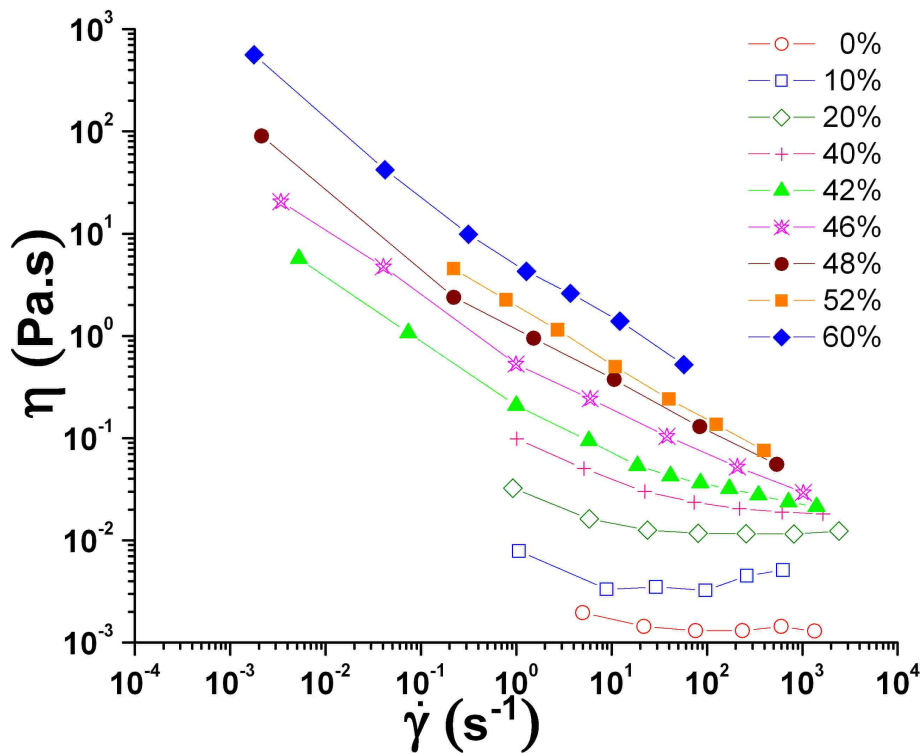


FIG. 1: Color online. Viscosity η (Pa.s) vs. shear rate $\dot{\gamma}$ (s^{-1}) at different volume concentrations ϕ from 0 to 60%

(G_0) determined by the value of $G'(f)$ at intermediate frequencies (1 Hz typically). The presence of elasticity has been observed previously for RBC suspensions [18], above a critical volume fraction around $\phi = 0.2$, and is believed to come from the elasticity of the cells as they are packed more closely at large concentrations such as the ones also encountered in tumour spheroids [14]. Finally, we observe that the trends in the $G' - G''$ plots for large concentrations ($\phi \geq 0.5$) are remarkably similar to previous microrheological results obtained on single cells [19, 20, 21]. Indeed, they show a slowly increasing G' and G'' (increasing slightly faster at frequencies above 1 Hz), where the elasticity dominates ($G' \geq G''$).

As in the case of suspensions, we define a maximum packing fraction ϕ_0 (which is usually 0.64 or even 0.74 for solid spheres in a face-centered-cubic crystal), depending on cell elasticity, i.e. their compactness [22]. Due to the presence of soft spherical cells, it is expected that the value of ϕ_0 will be in this range. ϕ_0 is determined using the reduced viscosity plot $\frac{\eta}{\eta_0}$ as a function of ϕ (η at a shear rate of $10^2 s^{-1}$, $\eta_0 = 0.0014 Pa.s$ the solvent viscosity). In

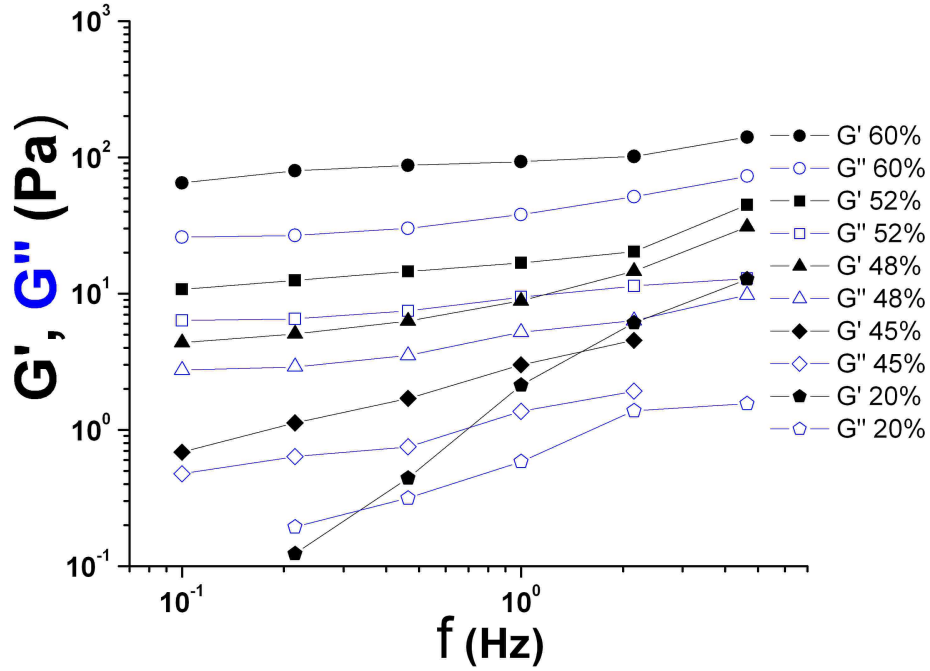


FIG. 2: Color online. Shear moduli G' and G'' (Pa) vs. frequency f at different volume concentrations ϕ ranging from 20% to 60%

our case, this data (not shown) is found to match the well-known equation

$$\frac{\eta}{\eta_0} = \left(1 - \frac{\phi}{\phi_0}\right)^{-2.5\phi_0} \quad (2)$$

proposed by Krieger and Dougherty [23], this providing the value $\phi_0 \sim 0.65$. Note that this relationship is interesting because it matches Einstein's viscosity for hard spheres [24, 25] $\eta/\eta_0 = 1 + 2.5\phi$ as well as Batchelor's correction for non colloidal spherical particles [26] $\eta/\eta_0 = 1 + 2.5\phi + 5.2\phi^2$ (here an expansion of (2) for small ϕ gives a second coefficient in the expansion of ~ 5 instead of 5.2, when using $\phi_0 = 0.65$). Finally, (2) diverges as expected when $\phi \rightarrow \phi_0$, the limiting packing fraction.

In order to investigate the effect of the volume concentration ϕ , we first need to obtain the flow curve $\sigma(\dot{\gamma})$ of the suspensions, as well as the relevant parameters, such as the yield stress σ_s . From the viscosity curve in Fig.1, we plot the stress $\sigma = \eta(\dot{\gamma})\dot{\gamma}$ vs. shear rate $\dot{\gamma}$ in Fig.3, and fit the data with the Herschel-Bulkley law [2] $\sigma = \sigma_s + M\dot{\gamma}^n$, where M is a constant, and n is a shear-thinning exponent ranging between 0 and 1 (1 is for a Bingham

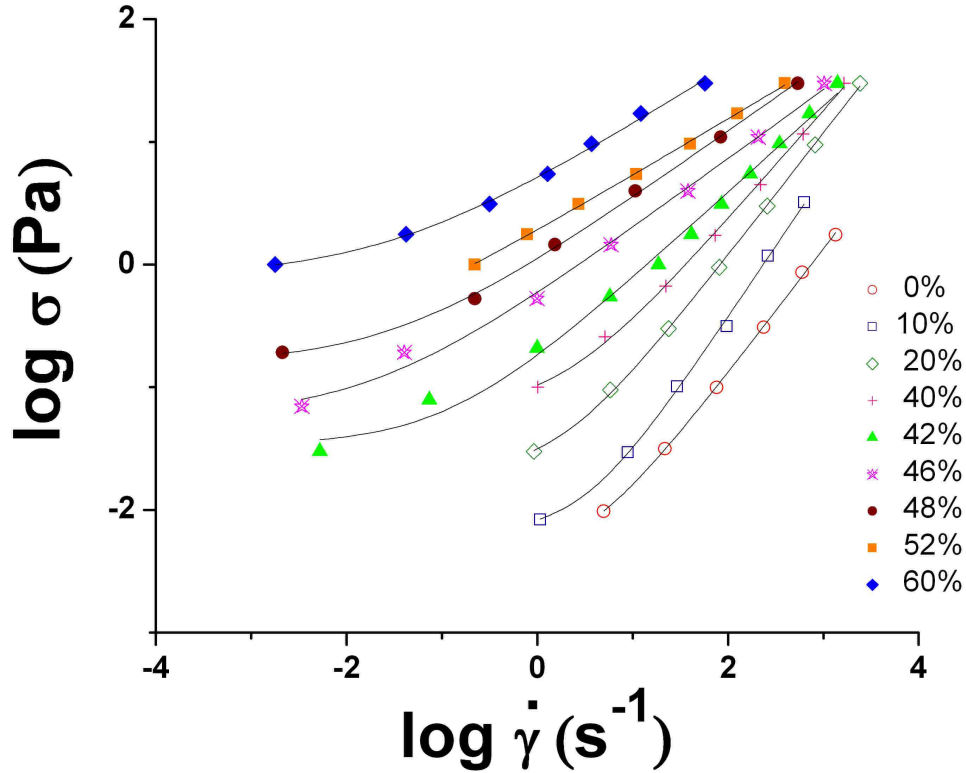


FIG. 3: Color online. Determination of the yield stress σ_s using Herschel–Bulkley’s model.

fluid, and the case of the Newtonian fluid is recovered for $n = 1$, $\sigma_s = 0$). Parameters have been optimized using a standard Newton–Raphson method. The parameter n is found to be very close to 1 at small concentrations (0, 10, 20 %) and decreases with concentration, taking respective values of 0.89, 0.71, 0.57, 0.55, 0.47, 0.47 for concentrations of 40, 42, 46, 48, 52 and 60 %. This point will be further discussed in §V.

This leads to the determination of the yield stress σ_s as a function of volume fraction ϕ . Such measurements are usually difficult [10] because of possible slip, sedimentation and evaporation [27]. Care has been taken to avoid such problems, therefore only shear rates larger than 10^{-3} s^{-1} (lowest value) are considered. The empirical Herschel–Bulkley model (involving a yield stress) is then used when sufficient data points are available. The fits are in satisfactory agreement with the data which gives good confidence in the values of the yield stresses for $\phi \geq 0.42$. Another attempt has been made using Casson’s model and gives similar data. The Bingham model was found to give less accurate values.

The values of the yield stresses σ_s and shear plateau moduli G_0 (value of G' at a typical

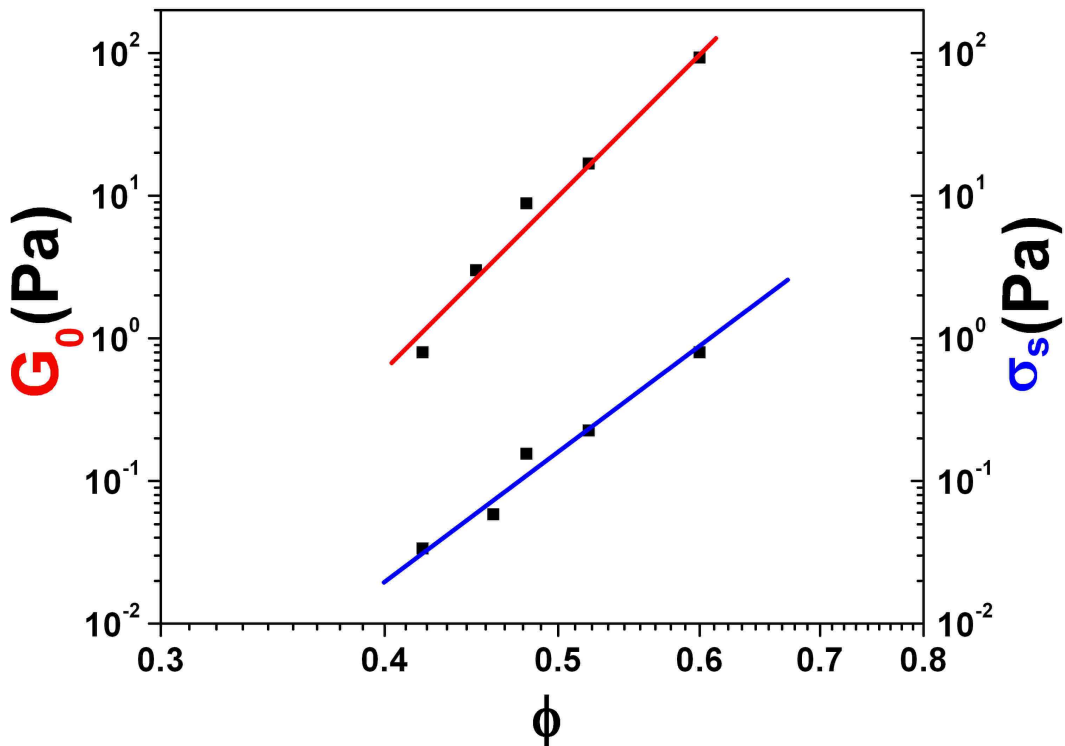


FIG. 4: Color online. Yield stress σ_s and Shear elastic modulus $G_0 = G'(f = 1Hz)$, vs. volume concentration ϕ , log-scale.

frequency $f = 1 Hz$) are plotted in Fig.4 as a function of volume concentration. This plot shows power law dependences of the form $\sigma_s \sim \phi^{m_1}$ and $G_0 \sim \phi^{m_2}$ and reminds previous results [11] obtained in the case of the rheology of RBCs suspensions, at least for the yield stress σ_s . From Fig.4 we find that $m_1 \sim 8.4$ and $m_2 \sim 11.6$. The m_1 exponent is quite different from the one obtained in the case of RBCs suspensions ($m_1 \sim 3$) as this will be discussed below.

IV. MODELLING

As seen above, rheological modelling of such suspensions should therefore predict shear-thinning behavior, as well as yield stress properties at low shear rates $\dot{\gamma} \rightarrow 0$ and a concentration dependence of σ_s and G_0 . In addition, cell suspensions correspond to aggregated systems (see Fig.5). Under flow, their structure is based on the persistent remodelling of

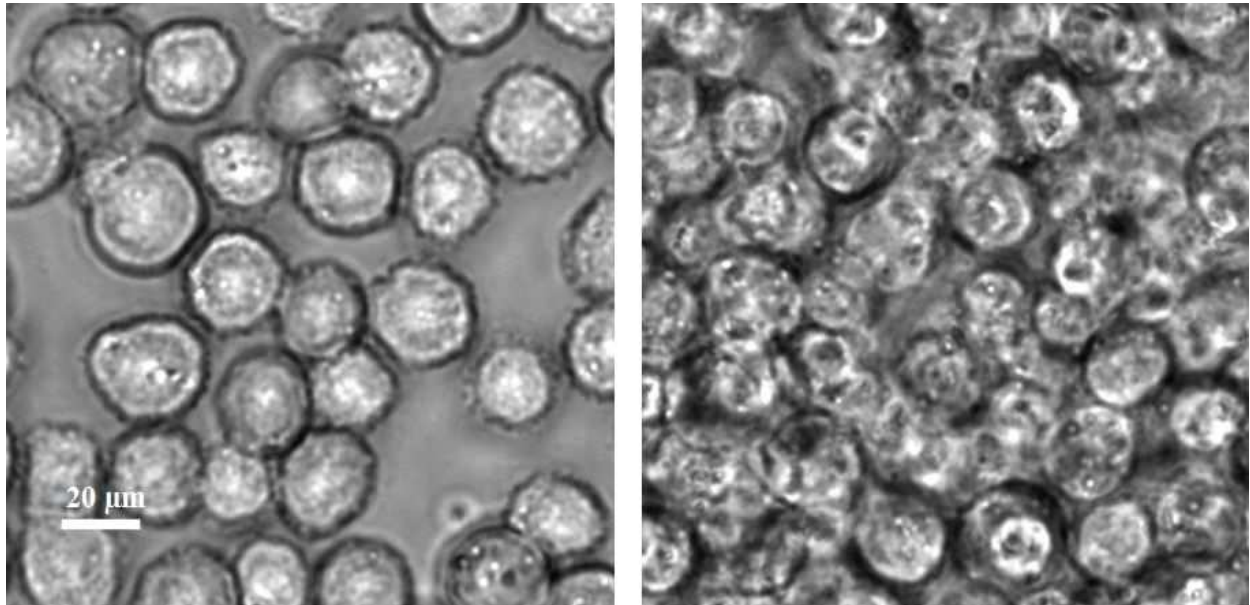


FIG. 5: Color online. Phase contrast microscopy of CHO cell suspension : 10% and 52%. Same scale for both images.

the cells with respect to each other as they exhibit deformations, rotations, possible rolling and/or separation. During such events, cells may form clusters of size R_f to be compared with the cell size a (radius). The formation and destruction of cell clusters is the major ingredient to understand the rheological properties of the cell system, in order to explain our data.

For example, when sheared under stress σ , clusters break into smaller ones, leading to shear-thinning effects. On the other hand, the possible encounter of clusters leads to the formation of larger structures, increasing the viscosity. Clusters are organized in a fractal way. First, one needs to consider a cluster at rest. Its size is R_f and it contains N cells, linked by the following relationship [28]:

$$\frac{R_f}{a} \sim N^{1/D} \quad (3)$$

where D is the fractal dimension. To determine D , we follow a previous approach [29] and consider circles (instead of rectangles) of radius R_f containing a cluster. Then cells (radius a) are counted for two rather small concentrations (10% and 20%). Clichés like the left one in Fig.5 are used to draw circles and count the number of cells N . For larger clusters containing more cells, we obtain a linear relationship between $\log_{10}(R_f/a)$ and $\log_{10}(N)$,

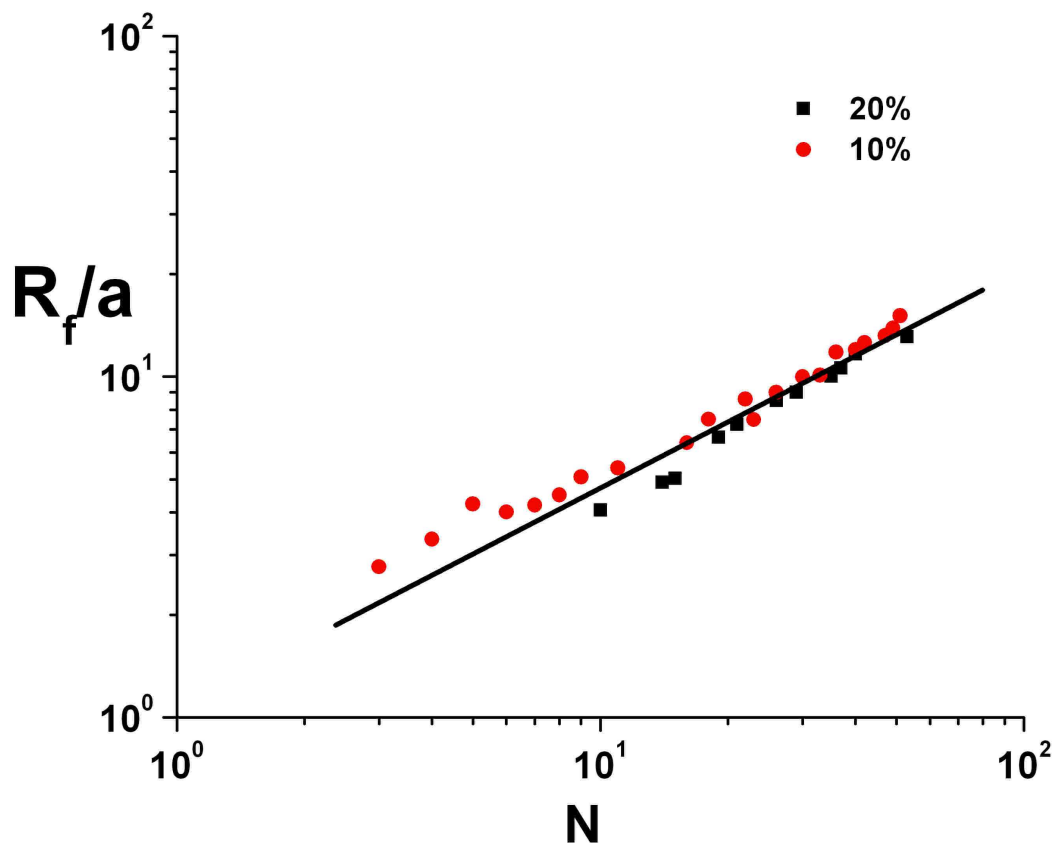


FIG. 6: Color online. Plot of $\frac{R_f}{a}$ as a function of N to determine the fractal dimension D . Two concentrations are used: 10% and 20%. There are noticeable differences at low values of N but there is an increased accuracy for large N , where the two concentrations give rise to the same slope. $D = 1.47$.

as shown in Fig.6. Note that the two cases studied (10% and 20%) give the same slope for large values of N , this justifying the fractal hypothesis indicated by equation (3). For our system, we determine $D \sim 1.47$ from the 2D images. Thus, in three dimensions, we expect a fractal dimension of the order $D \sim 2$ [30]. This number is similar to the ones found for RBCs suspensions, although the scaling exponents for yield stresses are quite different.

In the semi-empirical model proposed by Snabre and Mills [11, 12], the formation and dissociation of clusters under flow is taken into account. A change in R_f as a function of the applied shear stress is assumed :

$$\frac{R_f}{a} = 1 + \left(\frac{\sigma^*}{\sigma}\right)^m \quad (4)$$

where m is a dimensionless parameter. σ^* is a critical stress related to the interfacial adhesion between cells : $\sigma^* = \Gamma/a$, and Γ is the cell adhesion free energy. Using the concept of effective medium with volume fraction

$$\phi_A = \phi \left(\frac{R_f}{a}\right)^{3-D} \quad (5)$$

one assumes an effective viscosity :

$$\eta(\sigma) = \eta_0 \frac{1 - \phi_A}{\left(1 - \frac{\phi_A}{\phi_0}\right)^2} \quad (6)$$

and obtains the constitutive equation [31] which contains the yield stress given by :

$$\sigma_s \sim \sigma^* \left(\frac{\phi}{\phi_0}\right)^{\frac{1}{m(3-D)}} \quad (7)$$

The last parameter to be used in the formula, ϕ_0 , is the maximum packing concentration found previously.

We use the previous model to explain our experimental data. The exponent $m_1 = 8.4$ found for the yield stress σ_s is plugged into the previous scaling law (7) for determination of the parameter $m = 0.078$. This is smaller than the values of m found for RBC suspensions (typically $m \sim 0.3$). This means that the size of clusters is not so sensitive to the applied stress, indeed one can consider that the cell aggregates are easy to form (or hard to break) because of the round shape of the cells, in contrast with RBCs which need to bind in a very special way to form 'rouleaux'. Thus, once broken by stress, 'rouleaux' are difficult to reform. We have obtained the value of the critical stress $\sigma^* = 1.4 N/m^2$, and a corresponding value of $\Gamma = 1.4 \cdot 10^{-5} N/m$. This value of σ^* is higher than the ones obtained for RBCs [11] but the interfacial energy Γ is in the range of the small values indicated for vesicles [32]. This is in favor of the initial assumption that few adhesion molecules are involved in the region of contact between the cells.

Finally, we postulate a similar relationship [28] for the shear elastic modulus

$$G_0 \sim G^* \left(\frac{\phi}{\phi_0}\right)^{\frac{1}{p(3-D)}} \quad (8)$$

where G^* is an effective elastic modulus, but we include an additional exponent n to be determined. We come up with $p = 0.056$ and $G^* = 234Pa$. This value of the reference modulus G^* , as explained in the concept of fractal exponents [28], is to be related to typical values for single cells. In particular, it corresponds to a Young's elastic modulus $E^* = 702Pa$ (assuming that the cell is incompressible) which is typical for adherent Wild Type CHO cells, of the order $0.5 - 1 kPa$ as measured by AFM [33, 34].

V. AN APPROACH BASED ON STRUCTURAL SIMILARITY

Another method for having access to parameters like the yield stress σ_s and the viscosity η of such suspensions has been proposed earlier [17]. It can be of interest to mention such an approach since it is relevant to our case, in the context of concentration-dependent laws. The idea consists in assuming a dependence of the reduced shear stress $T = \sigma/\sigma_s$ as a function of the reduced shear rate $S = \eta\dot{\gamma}/\sigma_s$. This similarity is interesting because it can allow to superpose the different curves onto a single master curve. Such an approach has been used previously with success in the case of clay-water suspensions. The master curve is shown in our case for CHO cell suspensions (Fig.7).

We note again a good superposition of the data, although the few available data points for low reduced shear rates do not allow very accurate results for the parameters under investigation. In an attempt to model the first part of the curve (low shear rates), a relationship of the following kind was found :

$$T = 1 + 6.13 S^{0.47} \quad (9)$$

The value of the exponent close to $1/2$ recalls the well-known Casson's equation but in a slightly different form. In fact, this form is a limiting case of Casson's equation, corresponding to an asymptotic expansion of equation (1) for small enough shear rates. The use of equation (1) instead of (9) does not fit the whole data. Proceeding further, we can obtain values of the yield stress σ_s and viscosity η from the 'ad-hoc' data reduction. This has led us to similar relationships for the yield stress dependence vs. concentration (as in section IV). Similarly, the analysis of the viscosity (η) dependence against concentration ϕ also shows that equation (2) and the following equation $\eta/\eta_0 = [1 + 0.75/(\phi_0/\phi - 1)]^2$ from Chong and coauthors [35] both predict a correct evolution of the viscosity η leading to a

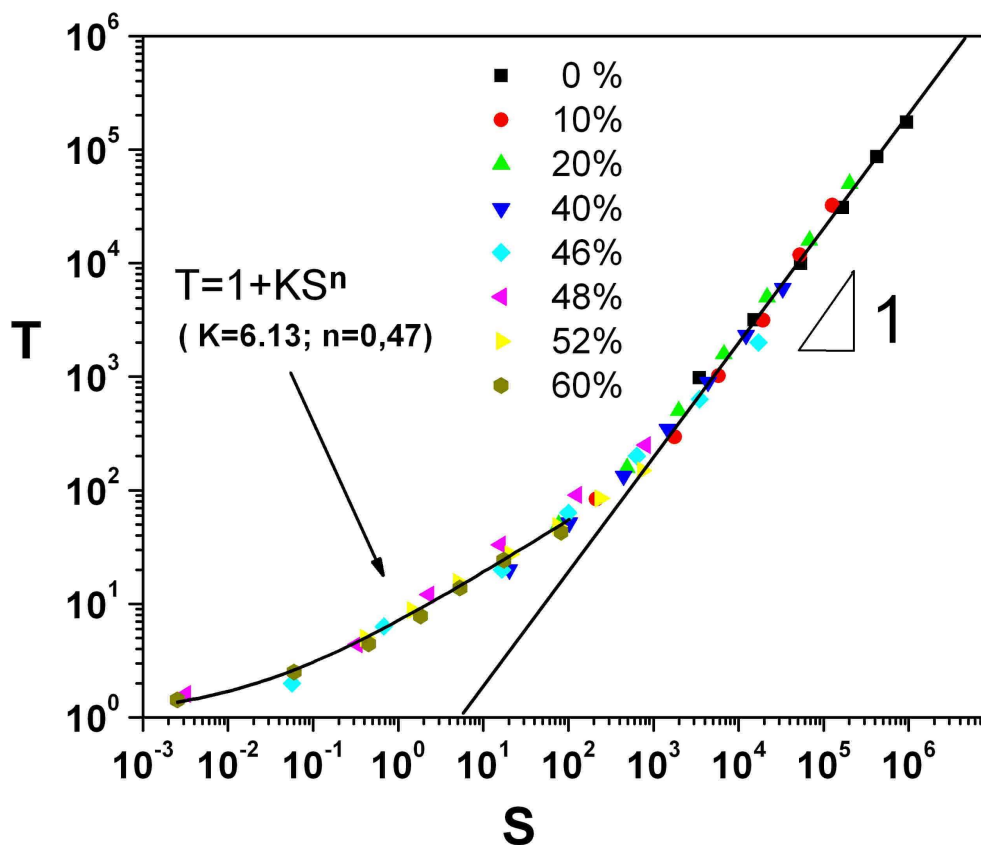


FIG. 7: Color online. Master curve of the reduced shear stress T vs. reduced shear-rate S .

packing fraction of the order $\phi_0 \sim 0.65$. Therefore we can conclude that this approach is complementary to the previous one in the sense that it can lead to an increased accuracy, when sufficient data is available, although it does not provide physical correlations between microscopic and macroscopic parameters, like the model that we chose to use in the above analysis [11].

VI. CONCLUSIONS AND PERSPECTIVES

To sum up, the system studied here provides unique features important for the rheology of biological suspensions and tissues. These concentrated cell suspensions behave as yield stress fluids (also called visco-plastic materials), for which a fractal approach has been used. Under shear, the fractal structure changes and can be modelled using a yield stress σ_s and

elasticity modulus G_0 related to the fractal dimension D . Two other microscopic parameters of interest have been introduced in the model: the cell adhesion energy Γ , and the cell's effective elastic modulus E^* found to be :

$$\Gamma \sim 10^{-5} N/m, E^* \sim 700 Pa \quad (10)$$

The first is in the range of typical values of cell adhesion energies, and the second in agreement with previous microrheology experiments. We also found a similar behavior between the dynamic shear moduli $G'(f)$ and $G''(f)$ in this study (at $\phi \geq 0.5$), and the ones obtained from microrheological studies on single cells [19, 20, 21] using various techniques. Both show slowly increasing dynamic moduli in terms of frequency, with the same relative positions. This idea probably deserves more attention and should be tested in the future, in particular further works may focus on the characterization of other cellular suspensions including cells with different elastic properties.

Finally, such a study can naturally lead to the understanding of biological tissues, by including stronger adhesion properties between the cells, or by taking into account the addition of Extra-Cellular Matrix components.

Acknowledgments – The authors wish to thank the EC Marie Curie Research Training Network MRTN-CT-2004-503661 on "Modelling, mathematical methods and computer simulation of tumour growth and therapy" (<http://calvino.polito.it/~mcrtn/>) for financial support, and C. Misbah for fruitful discussions about the manuscript.

-
- [1] R. G. Larson, *The structure and rheology of complex fluids* (Oxford University Press – New-York, 1999).
- [2] P. Coussot, *Rheometry of pastes, suspensions and granular materials* (Wiley - New York, 2005).
- [3] R. J. Flatt and P. Bowen, *J. Am. Ceram. Soc.* **89**, 1244 (2006).
- [4] A. N. Alexandrou and G. Georgiou, *J. Non-Newtonian Fluid Mech.* **142**, 199 (2007).
- [5] J. M. Brader, T. Voigtmann, M. E. Cates, and M. Fuchs, *Phys. Rev. Lett.* **98**, 058301 (2007).
- [6] H. M. Laun, *Angew. Makromol. Chem.* **124–125**, 335 (1984).
- [7] S. Chien, S. Usami, R. J. Dellenback, and M. I. Gregersen, *Science* **157**, 827 (1967).
- [8] S. Chien, S. Usami, R. J. Dellenback, M. I. Gregersen, L. B. Nanninga, and M. Mason-Guest, *Science* **157**, 829 (1967).
- [9] N. Casson, *A flow equation for pigment–oil suspensions of the printing ink type* (Pergamon–London, 1959), chap. 5.
- [10] S. Chien, S. Usami, H. M. Taylor, J. L. Lundberg, and M. I. Gregersen, *J. Appl. Physiology* **21**, 81 (1966).
- [11] P. Snabre and P. Mills, *J. Phys. III. France* **6**, 1811 (1996).
- [12] P. Snabre and P. Mills, *Colloids Surf. Physicochem. Eng. Aspects* **152**, 79 (1999).
- [13] D. Drasdo and S. Höhme, *Phys. Biol.* **2**, 133 (2005).
- [14] J. Galle, M. Loeffler, and D. Drasdo, *Biophys. J.* **88**, 62 (2005).
- [15] D. Ambrosi and L. Preziosi (2007), unpublished.
- [16] C. Verdier, *J. Theor. Medicine* **5**, 67 (2003).
- [17] P. Coussot, *Phys. Rev. Letters* **74**, 3971 (1995).
- [18] G. B. Thurston, *Biophys. J.* **12**, 1205 (1972).
- [19] B. Fabry, G. N. Maksym, J. P. Butler, M. Glogauer, D. Navajas, and J. J. Fredberg, *Phys. Rev. Lett.* **87**, 148102 (2001).
- [20] J. Alcaraz, L. Buscemi, M. Grabulosa, X. Trepast, B. Fabry, R. Farré, and D. Navajas, *Biophys. J.* **84**, 2071 (2003).
- [21] B. D. Hoffman, G. Massiera, K. M. V. Citters, and J. C. Crocker, *Proc. Natl Acad. Sci. USA* **103**, 10259 (2006).

- [22] D. Quemada, *Eur. Phys. J. AP* **1**, 119 (1998).
- [23] I. M. Krieger and T. J. Dougherty, *Trans. Soc. Rheology* **3**, 137 (1959).
- [24] A. Einstein, *Annals der Physik* **19**, 289 (1906).
- [25] A. Einstein, *Annals der Physik* **34**, 591 (1911).
- [26] G. K. Batchelor and J. T. Green, *J. Fluid Mech.* **56**, 401 (1972).
- [27] Y. C. Fung, *Biomechanics. Mechanical properties of living tissues* (Springer – New York, 1996).
- [28] P. G. de Gennes, *Scaling concepts in polymer physics* (Cornell University Press, 1979).
- [29] C. Allain and B. Jouhier, *J. Physique Lett.* **44**, 421 (1983).
- [30] M. Kolb and R. Jullien, *J. Physique Lett.* **45**, 977 (1984).
- [31] The 1D-constitutive equation is given by $\eta(\sigma) = \frac{\sigma}{\dot{\gamma}} = \eta_0 \frac{1 - \phi(1 + (\frac{\sigma_*}{\sigma})^m)^{3-D}}{(1 - \frac{\phi}{\phi_0}(1 + (\frac{\sigma_*}{\sigma})^m)^{3-D})^2}$ which is implicit for σ but provides an explicit relation for $\dot{\gamma}$ in terms of σ . Letting $\dot{\gamma} \rightarrow 0$ allows to determine the yield stress σ_s .
- [32] Z. Guttenberg, B. Lorz, E. Sackmann, and A. Boulbitch, *Europhys. Lett.* **54**, 826 (2001).
- [33] E. Canetta, A. Duperray, A. Leyrat, and C. Verdier, *Biorheology* **42**, 321 (2005).
- [34] M. Zhao, C. Srinivasan, D. J. Burgess, and B. D. Huey, *J. Mater. Res.* **21**, 1906 (2006).
- [35] J. S. Chong, E. B. Christiansen, and A. D. Baer, *J. Appl. Polym. Sci.* **15**, 2007 (1971).